

A COMPREHENSIVE 3D DYNAMIC MODEL OF THE HUMAN HEAD AND TRUNK

A. H. Vette^{1,2}, T. Yoshida^{1,2}, T. A. Thrasher³, and M. R. Popovic^{1,2}
¹University of Toronto, ²Toronto Rehabilitation Institute, ³University of Houston

INTRODUCTION

Linked-segment representations of the human body have been used extensively in biomechanics, ergonomics, and rehabilitation research to systemize thinking, make predictions, and suggest novel experiments [1]. In the particular scope of head and trunk biomechanics, they play an even more essential role as the dynamics of the spine are difficult to study *in vivo* compared to most other structures of the human body. Technical difficulties either preclude direct, yet non-invasive measurements of parameters (such as joint torques) or make experiments very time consuming and error prone [1,2]. As a result, mathematical modeling techniques are crucial for studying the dynamics of the upper body and to estimate joint torques and constraint forces for a wide range of scenarios.

In spite of the importance of upper body models, no study has reported on a universal yet detailed three-dimensional model of the upper body for estimating spinal joint torques and forces for different applications. As a result, researchers are still bound to develop and implement their own models of the upper body. Therefore, the objective of this study was to design a three-dimensional dynamic model of the upper body that is comprehensive and universally applicable for estimating spinal joint torques and forces from upper body kinematics ('inverse dynamics'). Specific requirements were that the model: (1) is flexible regarding the kinematic nature of the spinal joints (free, constrained, or fixed); (2) incorporates all geometric and mass-inertia parameters from a single, high-resolution source; and (3) can be implemented via different inverse dynamics formulations. To demonstrate its practicality, the model finally predicted the lumbar and cervical joint torques during perturbed sitting using experimental motion data.

GEOMETRIC MODELING

The proposed geometric model of the upper body focuses on the actions of the lumbar and cervical vertebrae, which are responsible for the majority of the spine and head movement [3]. The model, which is shown in Fig. 1, consisted of thirteen rigid bodies, representing five lumbar segments (L1 to L5), the thorax (TH), six cervical segments (C2 to C7), and the head portion adjacent to the C2 segment (HD). The lowest moving segment, i.e., the L5 segment, was located above the pelvis (PV), which marked the inertial frame of reference $\{F_{WD}\}$. Note that the inertial properties of the arms were incorporated into TH (Fig. 1).

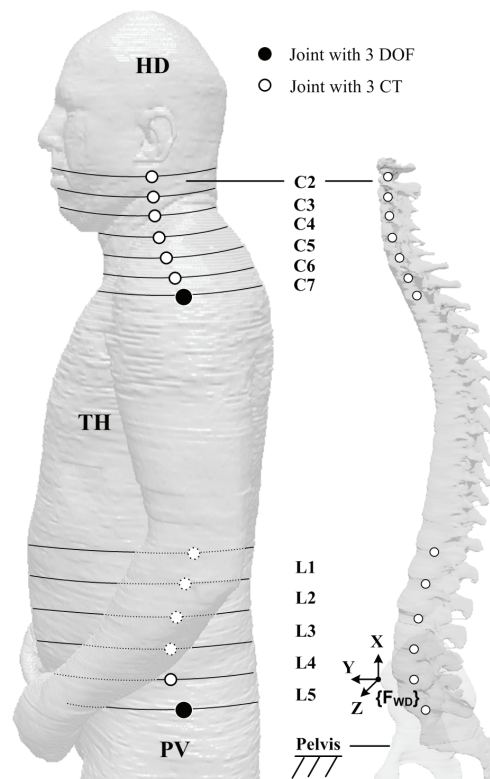


Fig. 1: Schematic representation of the geometric model of the upper body.

To accurately model upper body motion in three-dimensional (3D) space, the model had a total of six revolute degrees of freedom (DOF) and 33 revolute constraints (CT) that were located at the centers of thirteen intervertebral discs. The joints between the cervical and thoracic spine (C7-TH) and between the lumbar spine and the pelvis (L5-PV) had three DOF each, consisting of flexion-extension (FE), lateral bending (LB), and axial rotation (RT). The remaining cervical (HD-C2 to C6-C7) and lumbar (TH-L1 to L4-L5) joints were constrained to the motion of the 'DOF-joints' C7-TH and L5-PV, respectively. A particular CT's rotation was defined as a fraction of the rotation of the subjacent DOF-joint based on the two joints' ranges of motion as reported by White and Panjabi [4].

KINEMATIC MODELING

In order to identify the dynamic model and apply the inverse dynamics method, the kinematics of each model segment had to be described in local frames of reference ($\{F_{SEG}\}$). The frame assignment of the model, which is shown in Fig. 2, followed the Standard Denavit-Hartenberg notation [5].

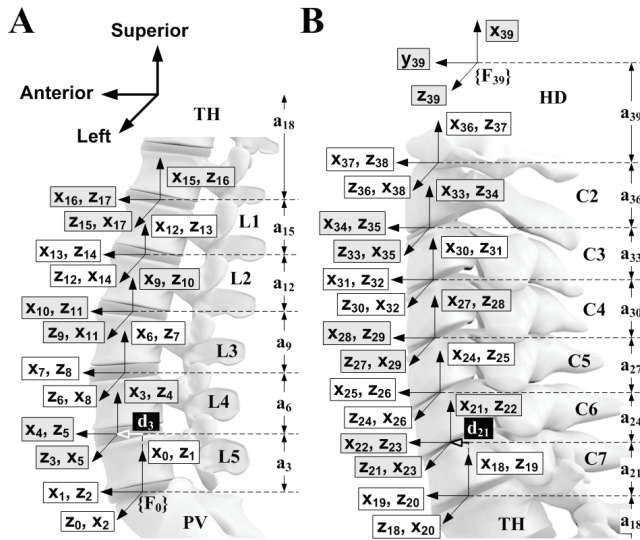


Fig. 2: Frame assignment to (A) the lumbar spine and (B) the cervical spine using the Standard Denavit-Hartenberg notation.

The required parameters consisted of the constant link lengths a_i , the constant link

offsets d_i , the constant twist angles α_i , and the time-varying revolute joint angles q_i . The quantities a_i and d_i represent the vertical and horizontal distances between the centers of the intervertebral discs, respectively, and were taken from the Male Visible Human (age: 38 years; height: 1.80 m; weight: 90 kg) as reported in our previous study [6]. The last frame $\{F_{39}\}$ was assigned to the vertex of the head, whereas the inertial coordinate frame $\{F_0\}$ represented a fixed translation of the world frame $\{F_{WD}\}$ to the L5-PV joint. All link parameters are listed in Table 1 (with $\alpha_i=90$ deg).

Table 1: Link parameters of the kinematic model (with $\alpha_i=90$ deg).

Joint axis	a_i [mm]	d_i [mm]	q_i [deg]	Motion
3	39.05	3.25	$90 + \theta_3$	L5-PV
6	38.91	-4.89	$90 + \theta_6$	L4-L5
9	38.78	-8.88	$90 + \theta_9$	L3-L4
12	35.76	-11.93	$90 + \theta_{12}$	L2-L3
15	35.81	-9.70	$90 + \theta_{15}$	L1-L2
18	295.77	17.05	$90 + \theta_{18}$	TH-L1
21	18.24	9.53	$90 + \theta_{21}$	C7-TH
24	17.11	4.91	$90 + \theta_{24}$	C6-C7
27	18.07	1.55	$90 + \theta_{27}$	C5-C6
30	18.05	-0.21	$90 + \theta_{30}$	C4-C5
33	19.10	1.62	$90 + \theta_{33}$	C3-C4
36	20.04	0.95	$90 + \theta_{36}$	C2-C3
39	172.66	-5.80	$90 + \theta_{39}$	HD-C2
other	0	0	$90 + \theta_i$	-

INVERSE DYNAMICS

To allow different constraint selections for the kinematic model shown in Fig. 2, all CT of the dynamic model were treated as DOF (13 joints with three DOF each). To calculate the spinal joint torques for upper body motion, the inverse dynamics of the model were implemented via (1) the Newton-Euler formulation (NE), (2) the Lagrangian formulation (LG), and (3) a block diagram within the commercial simulation environment Simulink (SM). NE and LG were developed in

Matlab (The MathWorks Inc., USA), whereas SM was realized using the SimMechanics blockset in Simulink (The MathWorks). Considering that experimental torque data from the spine are not easily available, using three different methods allowed us to ensure the internal validity of the results. The inverse dynamics formulations had the following commonalities:

- (1) three DOF per joint were implemented using a series of links with zero mass and zero length;
- (2) time derivatives of joint angles were obtained using the central difference scheme; and
- (3) the required mass-inertia characteristics were taken from the Male Visible Human [6].

APPLICATION: PERTURBED SITTING

Subject and experimental procedure

To demonstrate the practicality of the developed model, the inverse dynamics routines were used to predict the lumbar and cervical joint torques of one subject during perturbed sitting. The healthy male subject was 34 years of age, had very similar anthropometrics as the Male Visible Human (height: 1.80 m; weight: 89 kg), and reported no history of neuromuscular disorders or chronic back pain. He gave written informed consent to the experimental procedure, which was approved by the ethics committees of the University of Toronto and the Toronto Rehabilitation Institute in accordance with the declaration of Helsinki on the use of human subjects in experiments.

In agreement with past recommendations on motion data acquisition, two sets of four non-collinear markers were mounted on lightweight rigid panels and attached to the back of the subject's TH and HD. The subject was instructed to cross his arms lightly, close his eyes, and sit in a relaxed and natural upright posture. A total of 40 perturbation trials (eight horizontal directions, five trials each) were applied to the subject. Perturbations were delivered in the following directions, relative to the sagittal axis: 0° (anterior), 45°, 90° (right), 135°, 180° (posterior), 225°, 270° (left), and 315°. The order of the perturbation directions

was randomized to prevent anticipation, which has a significant effect on the perturbation response [7]. The horizontal perturbation had a Gaussian profile, a peak of approximately 200 N, and was applied just inferior to the axillae (T7 segment). The force and motion data were captured at 100 Hz using a load cell (MLP-100-CO-C, Transducer Techniques, USA) and an Optotrak 3020 motion analysis system (Northern Digital Inc., Canada), respectively.

Joint torque estimation

To execute the inverse dynamics calculations, a high-end personal computer with a 2.66 GHz processor was used. For a dataset with 500 samples (5-second trial), the computations took approximately 60 seconds for NE, 690 seconds for LG, and 5 seconds for SM (based on 14 executions each).

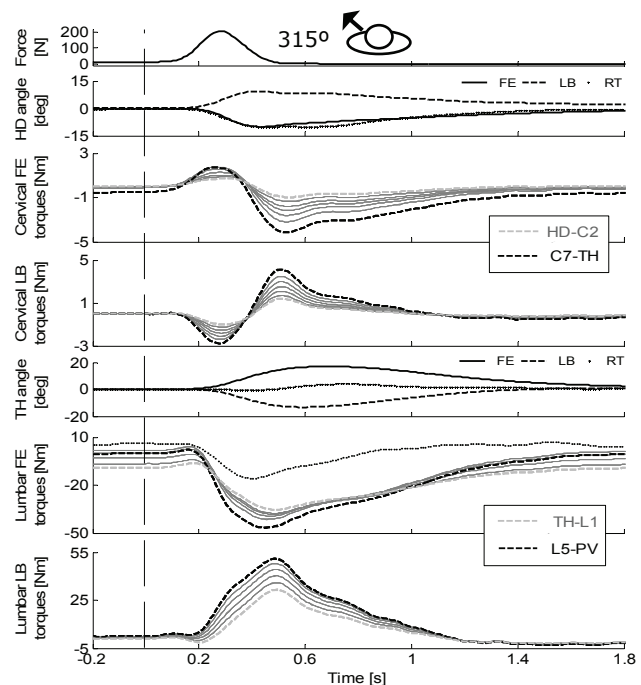


Fig. 3: Inverse dynamics results for perturbed sitting.

Fig. 3 depicts the inverse dynamics results for perturbed sitting. Shown are the average perturbation force, the average HD and TH angles, and the FE and LB torques (RT torques within ± 1 Nm) for an anterior-left diagonal perturbation (315°). In the torque plots, the

outputs from the three different inverse dynamics methods are plotted on top of each other. The dashed gray lines mark the predictions for the highest cervical and lumbar joints (HD-C2 and TH-L1), whereas the dashed black lines mark the predictions for the lowest cervical and lumbar joints (C7-TH and L5-PV). All other torques are shown using solid gray lines. In the second last subplot of Fig. 3 (lumbar FE torques), the thin dotted trace outlines the average electromyography (EMG) of the right erector spinae (at T9; rectified and low-pass-filtered; not to scale), demonstrating the involvement of active mechanisms in the balance stabilization act.

A simple visual inspection of Fig. 3 suggests that the joint torque estimates for NE, LG, and SM coincide. As this observation was supported by a coefficient of determination (R^2) of over 99.99999% for different time intervals, the internal validity of the inverse dynamics routines is confirmed.

DISCUSSION AND CONCLUSIONS

The perturbed sitting application demonstrates that the spinal joint torques can be easily identified using the developed inverse dynamics routines. In addition, since the three formulations were internally validated (R^2 of over 99.99999 % for different time intervals), researchers have different options for identifying spinal joint torques. While all routines can be feasibly implemented, each of them has its own advantages. For example, NE is not only comparably efficient, but also identifies the constraint forces between segments as needed for estimating spinal loading during various movements and tasks. Executing LG on the other hand is computationally more involved, but has the advantage of producing the system's kinetic and potential energies. Finally, SM represents more of a 'black box' approach, but is highly efficient and allows the user to quickly alternate between forward and inverse dynamics applications.

In summary, the present study takes advantage of the Visible Human Project to identify a detailed 3D dynamic model of the upper body that focuses on the action of the lumbar and cervical spine. The developed

model is particularly useful as it (1) is flexible regarding the kinematic nature of the cervical and lumbar joints (free, constrained, or fixed); (2) incorporates all geometric and mass-inertia parameters from a single, high-resolution source; and (3) can be feasibly implemented via different inverse dynamics formulations. Thus, this work directly responds to the postulation that structurally more complex and biologically more realistic models are needed to increase the accuracy of inverse dynamics computations [8]. Considering the growing importance of mathematical predictions, the developed model should become an important resource for researchers in different fields.

ACKNOWLEDGEMENTS

The authors thank Vivian Sin for her assistance in data acquisition and processing. This work was supported by the Canadian Institutes of Health Research, the Natural Sciences and Engineering Research Council of Canada, the Ontario Ministry of Health and Long-Term Care, the University of Toronto, and the Toronto Rehabilitation Institute.

REFERENCES

- [1] V. Goel and J. Weinstein, *Biomechanics of the spine: clinical and surgical perspective*, CRC Press, Boca Raton, Florida, USA, 1990.
- [2] L. Hansen et al., "Anatomy and biomechanics of the back muscles in the lumbar spine with reference to biomechanical modeling," *Spine*, vol. 31, pp. 1888-1899, 2006.
- [3] R. Preuss and J. Fung, "Musculature and biomechanics of the trunk in the maintenance of upright posture," *Journal of Electromyography and Kinesiology*, vol. 18, pp. 815-828, 2008.
- [4] A. White and M. Panjabi, *Clinical biomechanics of the spine*, 2nd Edition, Lippincott Williams & Wilkins, Philadelphia, Pennsylvania, USA, 1990.
- [5] J. Denavit and R. Hartenberg, "A kinematic notation for low-pair mechanisms based on matrices," *ASME Journal of Applied Mechanics*, vol. 23, pp. 215-221, 1955.
- [6] A. Vette, T. Yoshida, T. Thrasher, K. Masani, and M. Popovic, "A complete, non-lumped, and verifiable set of upper body segment parameters for three-dimensional dynamic modeling," *Medical Engineering and Physics*, vol. 33, pp. 70-79, 2011.
- [7] M. Gilles, A. Wing, and S. Kirker, "Lateral balance organisation in human stance in response to a random or predictable perturbation," *Experimental Brain Research*, vol. 124, pp. 137-144, 1999.
- [8] H. Hatzte, "The fundamental problem of myoskeletal inverse dynamics and its implications," *Journal of Biomechanics*, vol. 35, pp. 109-115, 2002.